Molecular Dynamics Simulation of Mixed Surfactants Adsorption on Graphene Nano-Sheets: Effects of Temperature, Electrolyte, and Alcohol

Poorsargol, Mahdiye*+; Poorgalavi, Masoomeh; Samareh Delarami, Hojat; Sanchooli, Mahmood; Karimi, Pouya

Department of Chemistry, Faculty of Science, University of Zabol, Zabol, I.R. IRAN

ABSTRACT: *An effective method for the preparation of stable dispersions of graphene is the direct exfoliation of graphene from graphite flakes in the aqueous solution of surfactants. Physical adsorption of surfactants on graphene surfaces is an important step in dispersing and stabilizing exfoliated graphene sheets in the aqueous medium. Dispersion of graphene with a mixture of surfactants is an effective way to obtain stable graphene sheets. The effect of synergism on a mixture of surfactants can reduce the total concentration of surfactants required for a particular application. The present study employed molecular dynamics simulation to investigate the adsorption of mixed cationic-rich and anionic-rich surfactants onto armchair graphene. We investigated the effects of temperature, electrolyte, and alcohol in the aqueous solution of surfactants on the adsorption process to understand the adsorption and self-assembly mechanism of surfactant mixtures on the graphene surface and also to better optimize the graphene dispersion process. The simulation results suggested the improved stability of these systems by adding an electrolyte to the aqueous solution of the surfactants. The screening effect of electrolyte ions on the electrostatic repulsion between groups of charged heads of surfactants has led to a denser accumulation of surfactants on graphene and more favorable interactions between them. Increasing temperature, however, reduced the system's stability by desorbing the mixed surfactants from the graphene surface. Comparing the surfactant molecules and graphene in terms of energy levels of Lennard-Jones interactions with and without alcohol also showed increased interactions in the absence of alcohol, which helps improve the system stability.*

KEYWORDS: *Graphene; Mixed surfactants; Dispersion; Molecular dynamics simulations; Adsorption.*

INTRODUCTION

Given the unique physiochemical properties of graphene and its extensive applications in nanotechnology, mass production of high-quality graphene has been high on the agenda in developing techniques [1-6]. The advantages of liquid-phase exfoliation using surfactants as the main graphene production technique include large-scale production of graphene using cost-effective graphite pieces and high-quality exfoliators as well as chemical functionalization of graphene [7-11]. As a limitation of this method, van der Waals (vdW) attraction between exfoliated

* *To whom correspondence should be addressed.*
+E-mail address: poorsargol.m@uoz.ac.ir
1021-9986/2022/12/3988-4003 16/$/6.06

graphene sheets in an aqueous solution decreases the concentration of single-layer graphene. Given the limited technological applications of graphene caused by the dispersion of graphene sheets into the solvent and its hydrophobic nature, surfactants are used to improve graphene dispersion [12]. Given that hydrophobic interactions between the surfactant tail and the graphene surface contribute to the adsorption of surfactants onto graphene, hydrophilic heads of surfactants are hydrated in an aqueous medium to obtain a stable graphene suspension [13-16]. Investigating the nature of cetyltrimethylammonium bromide (CTAB) interactions with graphene using ^{1}H Nuclear Overhauser Effect (NOE) Nuclear Magnetic Resonance techniques showed that CTAB chains have weak interactions with graphene nano-sheets [17]. These surfactant chains in quasi-bound states with graphene nano-sheets are rapidly exchanged with free surfactants in bulk.

The effects of various factors such as sonication time, centrifugation speed, the molecular structure of surfactants, surfactant concentration used, and the initial concentration of graphite on the concentration of graphene dispersed in solution were investigated [10, 12, 18-24]. Studies have shown that increasing the sonication time and force does not increase the concentration of dispersed graphene but damages them. The centrifuge speed should also be optimized to obtain the best quality dispersed graphene [10, 12, 19-20]. Examination of the effect of surfactants structure showed that the presence of benzene ring, C=C bond and longer alkyl chain in the structure of surfactants increases the ability of surfactants in graphene dispersion [21, 22, 25]. Moreover, the dispersion efficiency of gemini surfactants with double-chain alkyl structures was higher than that of single-chain surfactants [25]. *Díez-Pascual et al*. found out that the electrical resistivity, morphology, thermal stability, and microstructure of liquid exfoliated graphene can also be affected by surfactant's nature (non-ionic, cationic, and anionic) and chain length [26]. Their microscopic (Scanning electron microscopy and Atomic force microscopy) images showed a relation between the thickness of the graphene in the dispersions and the surfactant nature and chain length so that as the surfactant chain length increased, the flake thickness enlarged. In this regard, dispersions in non-ionic surfactants (e.g., non-ionic polyoxyethylene-23-lauryl ether (Brij L23)) differ from cationic or anionic ones (e.g., Sodium Dodecyl Sulfate (SDS) or CTAB) in that, the former exhibited the highest level of exfoliation, whereas the latter revealed fully-covered thicker sheets. The high and low Critical Micelle Concentrations (CMCs) of surfactant solutions have mostly been used for dispersion, and the surfactant's concentration used has been optimized in certain cases and the optimal values obtained were found to be very close to the CMC of the surfactant [27]. Recent studies have shown that a low surfactant concentration approaching the surface aggregation concentration (instead of a high CMC) produces a high graphene concentration, but this accomplishment requires the use of surface tension-reducing agents (such as alcohols) [28]. Given the concerns about the cost and environmental impact of surfactants, it is important to find a way to obtain more dispersed graphene using smaller amounts of surfactant.

Pure surfactants differ from their mixture in behavior; for instance, synergistic interactions (attractions) between head groups lower CMCs in catanionic mixtures compared to in pure surfactants as their constituents [29-30]. The synergistic behavior of mixed surfactants can decrease their overall concentration. Using catanionic mixtures comprising SDS and CTAB showed the effectiveness of cationic-rich and anionic-rich mixtures in dispersing graphene [31]. The synergistic effect in the catanionic mixtures decreased the required concentrations of the surfactants used to disperse graphene compared to that of pure surfactants. Using mixed surfactants to disperse graphene can also help decrease environmental effects and costs.

The effect of electrolytes on the adsorption of surfactants on solid surfaces was investigated and revealed that the addition of electrolytes to aqueous solution increases the adsorption of ionic surfactants on silica surfaces [32, 33]. Electrolyte has a screening effect on the electrostatic repulsion between surfactant head groups. Therefore, head groups approach one another and surfactants are further packed onto surfaces. According to finding *Silvera-Batista et al*., the presence of electrolytes improves the structure of surfactants on the surface of SWNTs, leading to the preservation of Single-Walled Carbon NanoTubes (SWNTs) suspended by SDS on agarose gels [33]. Electrolytes can also affect the interfacial structures of surfactants on graphite surfaces, and increasing electrolyte concentration reduces the distance between the assemblies of surfactants adsorbed onto graphite surfaces [34]. The effect of alcohol as a surface tension-reducing agent on graphite exfoliation

with SDS surfactant was investigated by *Yeon et al* [28]. They showed that more graphene dispersion could be obtained with lower levels of surfactant provided that the surface tension of the solution was maintained by alcohols at about 41.0 mN/ml. Dispersion of Multi-Walled Carbon Nanotubes (MWCNTs) in ethanol solvent was also investigated using SDS, Triton X-100, Span-60, Pluronic F-127, and CTAB surfactants [35]. UV-Vis spectroscopy, zeta-potential, and transmission electron microscopy results showed that SDS and Span-60 have a higher dispersing ability thanks to their functional and geometric groups. The hydrogen bonds between hydroxyl (OH) functional groups and MWCNTs carboxylic acids (-COOH) functional groups cause the wetting of the CNTs hydrophobic surface and thus the unbundling and dispersion of the CNTs. *Lund et al*. used Sodium Cholate (SC) surfactant to exfoliate high-shear graphite with temperature control and synthesized high concentrations of 3 mg/mL high-quality graphene only after 2 h of exfoliation shear [36]. They emphasized that this high concentration is due to the selection of suitable mixing parameters such as low exfoliation temperature (10 °C) and proper surfactant concentration. They observed that after 15 minutes of mixing, the concentration of dispersed graphene at 10 °C was twice that of dispersed graphene at 50 °C. Therefore, lowering the temperature during exfoliation increases the concentration of dispersed graphene. It was shown that higher graphene concentrations at 10 °C were correlated with better adsorption of SC molecules on dispersed graphene surfaces at this temperature. In addition, graphene-SC dispersions can be more stable at low temperatures due to the reduced mobility of graphene plates and free surfactants. Recently, Khosravian and Javadian used the bio-surfactant Docosahexaenoic acid (DHA) for liquid phase exfoliation graphite and investigated the self-assembly morphology of this surfactant and the effect of pH and the number of layers using MD and Symmetry Adapted Perturbation Theory (SAPT) [37]. They observed that reducing the medium's pH increases electrostatic attraction interactions between surfactants, which leads to the instability of colloidal dispersions and demonstrates the important role of pH in the dispersion process. Investigating the effect of number of layers showed that the initial force for the liquid phase exfoliation is created by sonication, and exfoliation cannot start without an ultrasonic aid. The repulsive force between surfactant head-groups then keeps the graphene layers separate from each other.

Computer simulation is a powerful data collecting tool at microscopic level on the systems being examined [38-49]. This method facilitates the study of cases that are experimentally time-consuming, costly or impossible. In addition, simulation results reduce the number of experimental trails and errors. MD is used to investigate the molecular structure and concentration of surfactants and their adsorbed amount and structure on nanoparticles and interactions between their molecules and nanoparticles [13-16, 25, 31, 38, 50-51]. Microscopic simulations provide valuable information about the self-assemblies of ionic and non-ionic surfactants on the graphene surface and the self-assembly structure of surfactants in different situations. Effects of surfactant concentration on the self-assembly morphology, surfactant structure, graphene nano-sheets size and shape, the number of graphene layers and the interactions between two surfactant-coated graphene nano-sheets have been investigated as the most important parameters of simulations. The potential mean force simulations were used to characterize the stability of graphene and investigate the interactions between liquid-phase graphenes, including elegant interplays between different interfacial forces such as electrostatic and vdW forces arising from surfactants confined between graphene sheets, repulsive steric forces and the forces caused by couterions in ionic surfactant solutions [8, 14, 31].

The present study conducted all-atom MD simulations to investigate the adsorption of mixed surfactants onto graphene nano-sheets under different conditions. The effects of temperature, electrolyte and alcohol on the adsorption and morphology of the assemblies formed on graphene sheets were also investigated. The findings can help optimally use a mixture of surfactants in dispersing graphene. The synergistic effect of the mixture of surfactants can reduce the total concentration of surfactants required in a particular application. Using electrolytes and alcohol in combination with mixture of surfactants can also significantly reduce the concentration of surfactants required for graphene dispersion. Therefore, these factors together can reduce both costs and environmental effects of surfactants. MD simulation can be helpful for experimentalists who wish to understand a theory's abilities, and how a theory can cooperate in providing the insight needed for dispersion process comprehension and the design and optimization of dispersion methods.

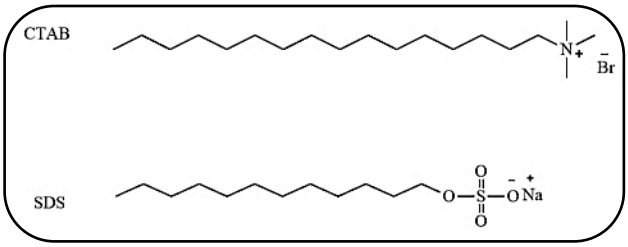

Fig. 1: The chemical structure of surfactants used in the present study.

SIMULATION METHOD

GROMACS 2018 is used to simulate the adsorption of surfactant mixtures onto graphene under different conditions [52]. A 5×5 nm^2 single-layer graphene was fixed in the center of a box during the simulation by applying a force of 1000 $kJ/mol.nm^2$. The non-bonded Lennard-Jones (L-J) parameters used for the naphthalenation of carbon atoms in the OPLS-AA force field were employed to model all the graphene carbon atoms as uncharged L-J spheres [53]. The SDS and CTAB molecules were modeled using the OPLS-AA force field and the water molecules using the standard SPC/E model [54]. SDS surfactant is an anionic surfactant with a negatively charged head group in its structure. SDS surfactant contains an anionic sulfate functional group. CTAB surfactant is a cationic surfactant with a positively charged head group in its structure. CTAB surfactant contains the cationic trimethylammonium functional group. Fig. 1 shows the chemical structure of the study surfactants. Long-range electrostatic interactions were calculated using the particle mesh Ewald (PME) method [55]. A 1.2-nm cut-off distance was considered for vdW interactions. Verlet integration with a time step of 2 fs and a Nose-Hoover thermostat were used to conduct the simulations in the isothermal-isobaric ensemble at 300 and 600 K [56-57]. The Parrinello-Rahman barostat was used to maintain the pressure at 1 bar [58]. Periodic boundary conditions were considered in all the three directions, and trajectories, velocities and forces on the constituent atoms of the system were stored every 10 ps.

According to Fig. 2, the molecules of the surfactants were initially oriented perpendicular to the graphene surface in PACKMOL to decrease the simulation time [59]. This structure is commonly used to simulate SDS assemblies on SWNTs and graphite [60-61]. The final self-assembly structure obtained from this vertical configuration was the same as that obtained from random initial configurations [14, 15, 25, 31, 60-61]. The simulation box was then filled with water molecules. The simulations were performed at 300 and 600 K to investigate the effect of temperature on the adsorption and morphology of the assemblies formed on the graphene surface. The effect of electrolyte on the adsorption of the surfactant mixture onto graphene was evaluated using 4M NaCl electrolyte for each of the study systems. Ethanol in the aqueous solution was also evaluated in terms of its effects on the mixed surfactants. The simulated systems were detailed in Table 1 by presenting temperature, the total simulation time and the total numbers of SDS, CTAB, water, NaCl and ethanol molecules. It should be noted that the surface coverage used in this study and the simulation time is comparable to the surface coverage and the simulation time in other simulation studies on graphene dispersion using surfactants [14, 15, 25, 31, 60-61].

The steepest descent method was used to minimize energy levels before beginning the MD simulations. The systems reached equilibrium within 11 ns and the data were analyzed within the final 8 ns of the simulation. Visual MD (VMD) was employed to obtain the structural images [62]. VMD is a computer program for molecular modeling, visualization, and analysis of biological systems like proteins, nucleic acids, and lipid bilayer assemblies. VMD is also used to view more general molecules, as VMD can read standard protein data bank (PDB) files and display the structured content of the file. VMD has a variety of methods for rendering and staining a molecule: simple dots and lines, CPK spheres and cylinders, licorice joints, backbone tubes and ribbons, cartoon drawings, etc. VMD also provides animation and trajectory path analysis of a MD simulation. In this study, we used VMD to visualize the structures because of the PDB files used in this study.

RESULTS AND DISCUSSION

Equilibrium State

The Root Mean Square Deviation (RMSD) curves in Fig. 3 used to determine the equilibrium states of the system before data collection gradually increased in the first 3 ns and reached a plateau or equilibrium within the final 8 ns. These curves confirmed the adequacy of the simulation time used to determine the equilibrium of all the systems. The system properties were specified after reaching equilibrium.

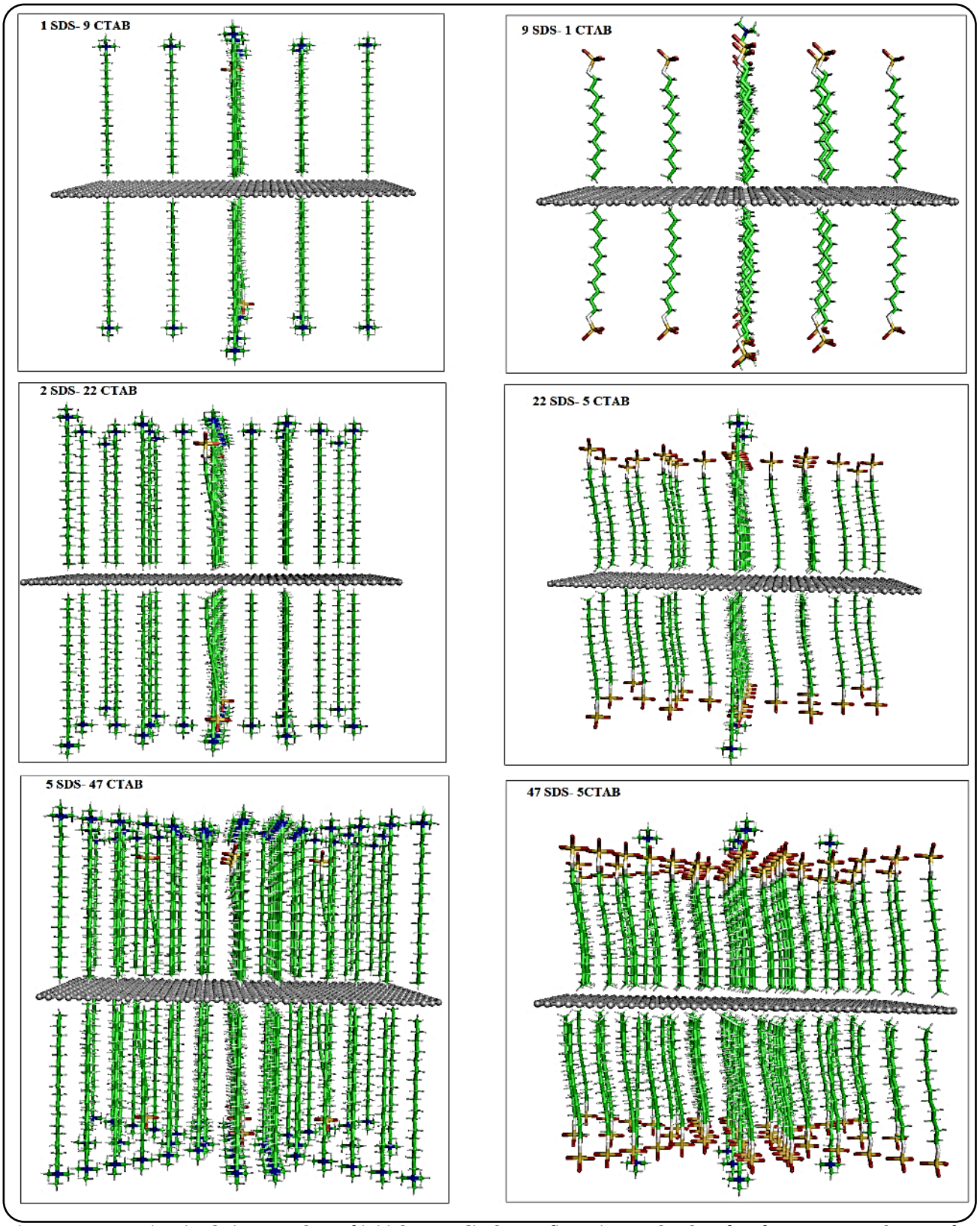

Fig. 2: Representative simulation snapshots of initial perpendicular configurations molecules of surfactants on graphene surface before equilibrium. Water molecules are not shown for clarity. Color code: blue, nitrogen; white, hydrogen; green, carbon atoms in CTA^+ and DS^- ions; red, oxygen; yellow, sulfur; and silver, graphene carbon.

Table 1: Details of the simulated systems.

System	Number of SDS	Number of CTAB	Number of water	Number of NaCl	Number of ethanol	temperature	Simulation time (ns)
1	2	18	12548 (12548)	-	-	300 (600)	11
2	18	2	12621 (12621)	-	-	300 (600)	11
3	4	44	11963 (11963)	-	-	300 (600)	11
4	44	4	12157 (12157)	-	-	300 (600)	11
5	10	94	11066 (11066)	-	-	300 (600)	11
6	94	10	11383 (11383)	-	-	300 (600)	11
7	2	18	10596	976	-	300	11
8	18	2	10669	976	-	300	11
9	4	44	10011	976	-	300	11
10	44	4	10205	976	-	300	11
11	10	94	9114	976	-	300	11
12	94	10	9431	976	-	300	11
13	2	18	11616	-	250	300	11
14	18	2	11688	-	250	300	11
15	4	44	11040	-	250	300	11
16	44	4	11227	-	250	300	11
17	10	94	10160	-	250	300	11
18	94	10	10469	-	250	300	11

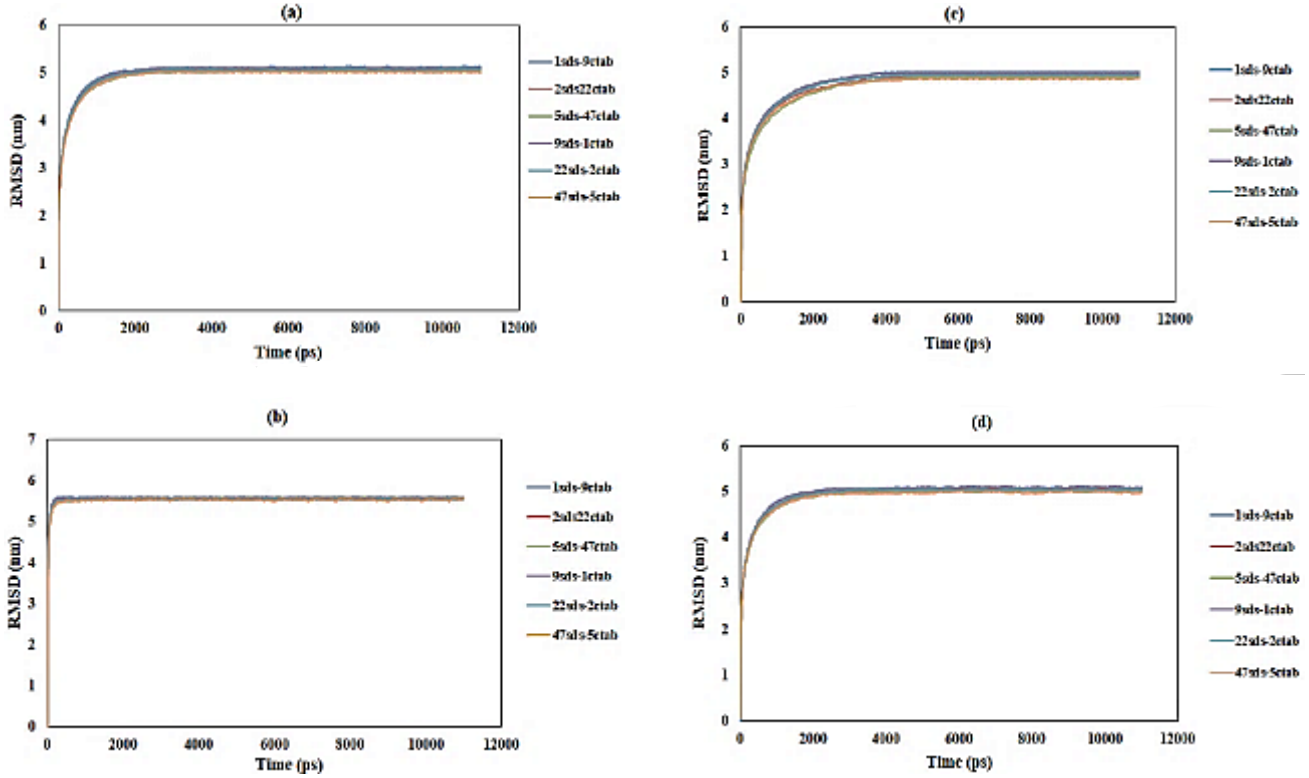

Fig. 3: RMSD curves for the simulated systems (a) in temperature 300 K (b) in temperature 600 K (c) with 4M NaCl electrolyte and (d) with ethanol as a function of simulation time. As shown, the curves are flatted after about 3 ns, suggesting that the systems have reached equilibrium. Thus, data analysis was carried out in the last 8 ns of the simulation.

Effects of temperature

The simulations were performed at 300 and 600 K to evaluate the effect of temperature on the adsorption of the mixed surfactants onto graphene nano-sheets. Fig. 4 shows the snapshots of the adsorption onto single-layer graphene sheets at these temperatures, suggesting higher adsorption levels and more regular molecular orientation on the graphene surface at the lower temperature. There space on the graphene surface was adequate at a low and medium surface coverage and molecules were adsorbed in parallel forming a single-layer structure. This orientation exposed the hydrophobic tails of the surfactants to the aqueous solution and their hydrophilic heads to the hydrophobic graphene surface, which reinforced hydrophobic interactions between the tails of the surfactants and graphene and stabilized the graphene-surfactant structure. This orientation of SDS/CTAB molecules on graphene is similar to the orientation of SC surfactant molecules on graphene [14]. At a high surface coverage, the inadequate space on the graphene surface increased repulsive forces between the molecules. Most of the surfactant molecules on the graphene surface are bent and their hydrophilic heads tend toward the aqueous phase to reduce these forces. Increased hydrophobic interactions between the tails of the surfactants and the graphene surface also helped stabilize the graphene-surfactant structure. Moreover, hemi-spherical structures formed as a result of significant changes in the orientation of the surfactant molecules on the graphene surface. Single-layer and hemi-spherical structures on graphene have already been observed in graphene dispersion simulations using SC, SDS, and CTAB surfactants [14, 15, 63]. Comparison of simulation snapshots at 300 and 600 K shows that the adsorption of surfactants on graphene at low temperatures is complete, while the adsorption is not complete at high temperatures and some surfactant molecules are dispersed in the simulation box. This observation is in line with the results of *Lund et al*., who showed that better absorption of SC molecules on dispersed graphene surfaces occurs at lower temperatures [36].

The total energy is the sum of kinetic energy and potential energy calculated in each step of the simulation. The momentary kinetic energy depends on the velocity of particles, and the velocity of all the particles in each simulation step is determined by numerical integration of Newton's equations of motion [64]. Then, by calculating the mean of momentary kinetic energy, its value is obtained for the system. The potential energy is also calculated by calculating the mean of its momentary values in different simulation steps. This quantity, which yields the forces, is calculated during the simulation in each step. Therefore, the potential energy indicates the interactions between the particles in the simulation system. Since the total energy during the simulation is continuously converted from kinetic energy to potential energy and vice versa, more negative values of the total energy indicate more favorable interactions between the particles in the simulation system. Surfactant and sheet graphene molecules are components in our simulated systems where surfactant molecules interact with graphene sheets together. Table 2 presents the total energy levels of the simulated systems at 300 and 600 K. As Table 2 shows, the total energy for the systems at 300 K is more negative than the total energy for the systems at 600 K, denoting that the interactions between these particles are more desirable in 300 K systems.

A set of mathematical equations are used to express intermolecular forces in computer simulations. The L-J potential is an intermolecular potential model that most simulations use to describe simple intermolecular interactions. The L-J potential describes the potential energy of the interaction between two atoms or non-bonded molecules based on their separation distance. The L-J potential models the repulsion and attraction interactions between atoms or non-ionic molecules. Two interacting particles repel each other at close distances, attract each other at medium distances, and have no interaction at infinite distances. The L-J potential is represented by the following equation:

$$V_{LJ}(r) = 4\varepsilon \left[\left(\frac{\delta}{r}\right)^{12} - \left(\frac{\delta}{r}\right)^{6} \right] \quad (1)$$

where V_{LJ} is the intermolecular potential between two particles, r is the distance between the two interacting particles, ε is the depth of the potential well (a measure of how much the two particles attract each other), and δ is the distance at which the particle-particle potential energy (V_{LJ}) is zero. The first part of Equation $(\delta/r)^{12}$ describes repulsive forces between particles, while the second part $(\delta/r)^{6}$ describes attraction [65]. Table 3 shows the energy levels of L-J interactions between the mixed surfactant molecules and graphene at these temperatures. The lower

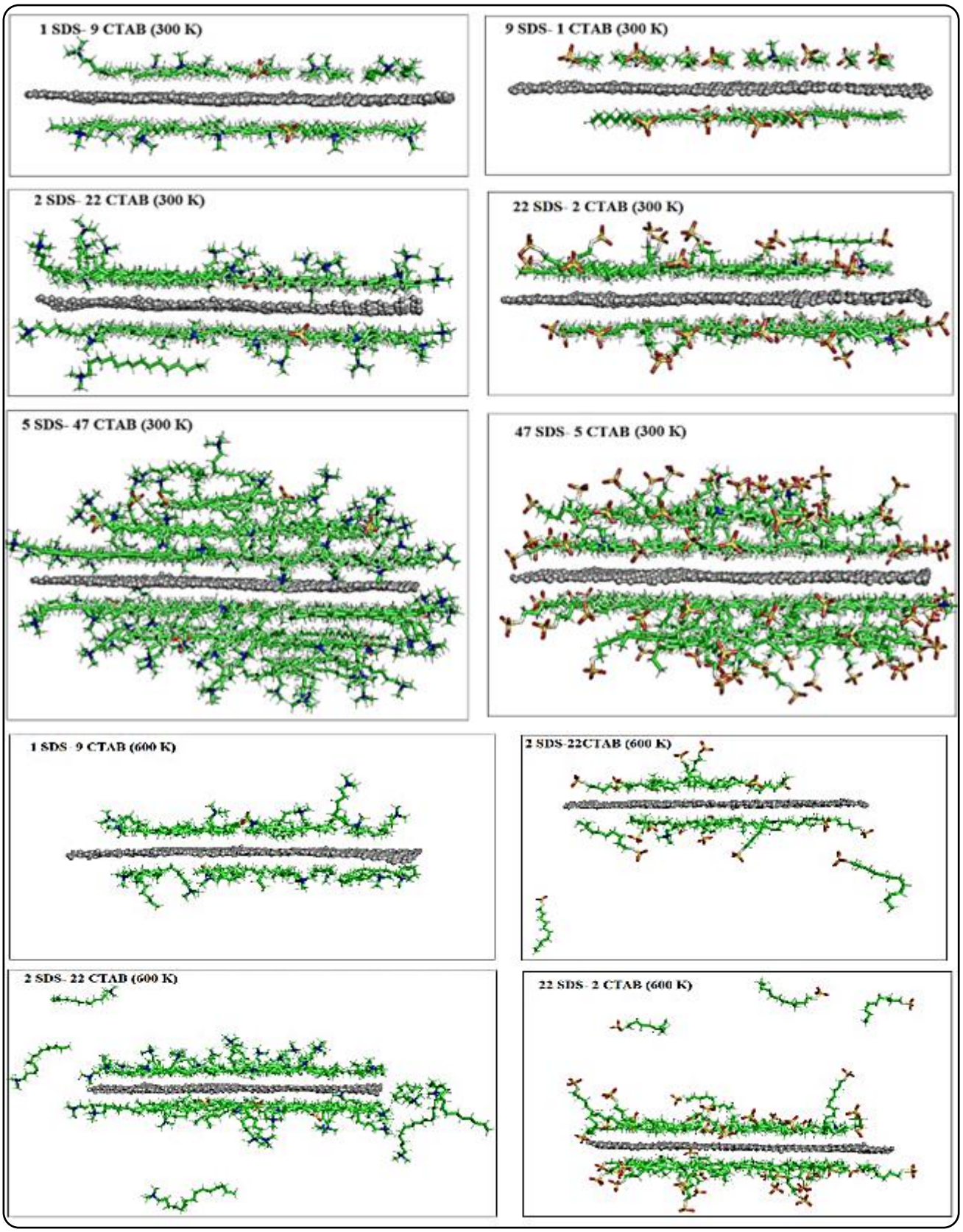
1 SDS- 9 CTAB (300 K)
9 SDS- 1 CTAB (300 K)
2 SDS- 22 CTAB (300 K)
22 SDS- 2 CTAB (300 K)
5 SDS- 47 CTAB (300 K)
47 SDS- 5 CTAB (300 K)
1 SDS- 9 CTAB (600 K)
2 SDS-22CTAB (600 K)
2 SDS- 22 CTAB (600 K)
22 SDS- 2 CTAB (600 K)

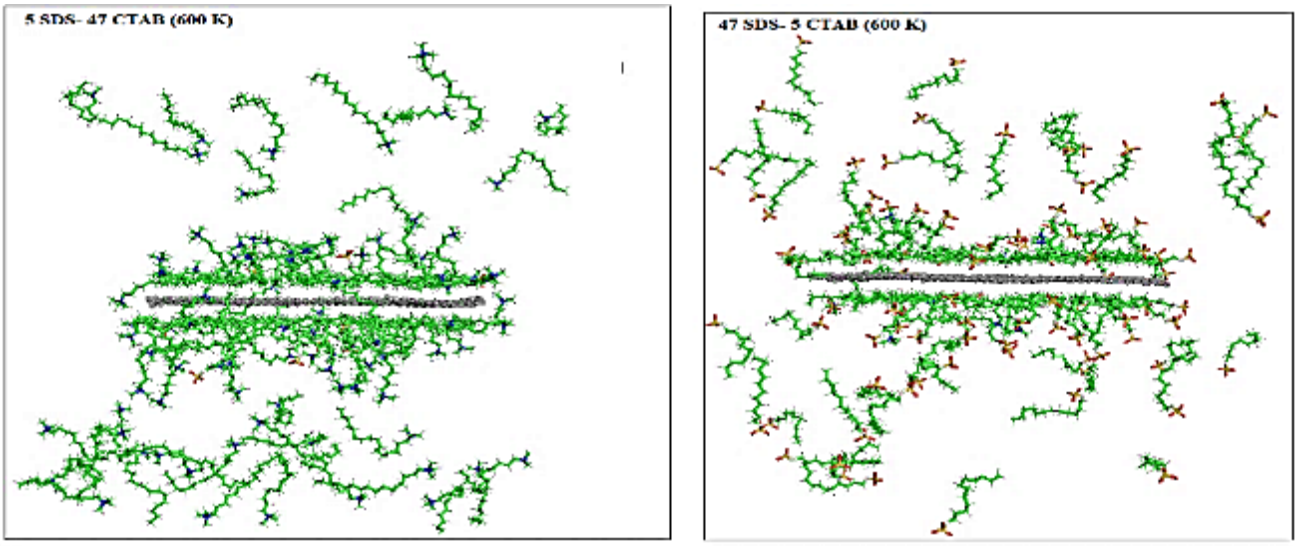

Fig. 4: Representative final equilibrium simulation snapshots of adsorption of mixed surfactants onto single-layer graphene sheets in temperatures 300 and 600 K. Water molecules are not shown for clarity. The color code is the same as in Fig. 2.

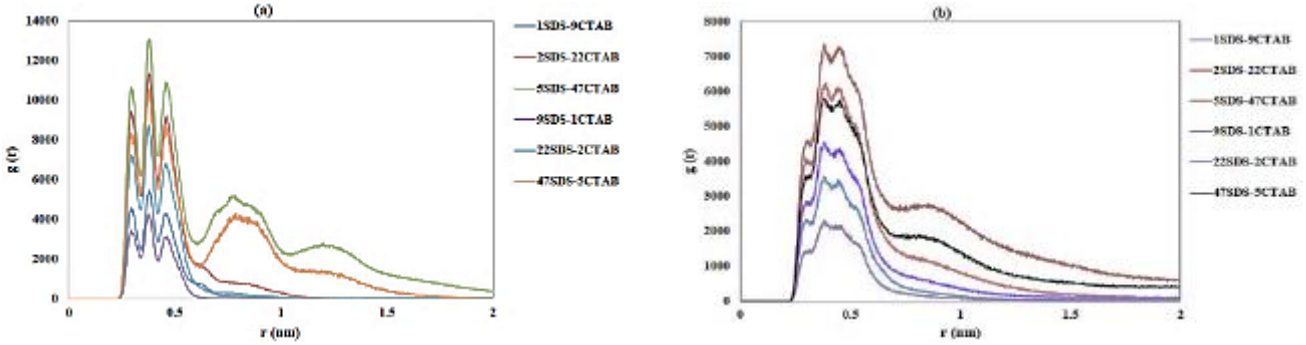

Fig. 5: Simulated radial distribution functions (RDFs) of surfactants as a function of the distance from the z-axis of the graphene in temperatures (a) 300 K and (b) 600 K.

the temperature, the lower the energy levels, the higher the interaction stability and the higher the amount of surfactant adsorbed onto graphene. Table 4 shows the higher kinetic energy of the simulated systems at 600 compared to 300 K. This temperature-dependent increase in the kinetic energy of the surfactant molecules moved them away from the graphene surface and decreased their adsorption. Comparison of the L-J and kinetic energy values of the simulated systems at 300 and 600 K showed the greater stability of graphene-surfactant dispersions and the lower mobility of surfactants at lower temperatures. It has already been shown that graphene-SC dispersions at low temperatures can be more stable than graphene-SC dispersions at high temperatures due to the reduced mobility of graphene and surfactants [36].

The Radial Distribution Function (RDF) or correlation pair function denoted as g(r) shows the distribution of atoms (molecules) around a particular atom (molecule) and the local structure of the system. As a function of the system temperature and density, g(r) can help determine the probability of identifying a particle within radius r of a reference particle. This function can be derived from the simulations by locating single atoms as a function of time based on MD paths. The RDF can be used to obtain the adsorption rate and the distribution of surfactants adsorbed on graphene and locate surfactant molecules around graphene nano-sheets. Fig. 5 shows the RDF of the surfactants with respect to the graphene axis at 300 and 600 K. Comparing Fig. 5a with 5b shows the higher adsorption rate of the surfactants on graphene at 300 K. The strongest peak observed at about 0.4 nm showed physisorption and the closest surfactant molecules to the graphene surface.

Table 2. The mean values of total energy (kJ/mol) for all simulated systems.

System	300 K	600 K	NaCl	Ethanol
1SDS-9CTAB	-478020.58	-164699.62	-1135851.38	-437317.98
2SDS-22CTAB	-454375.95	-139242.08	-1113112.50	-413967.43
5SDS-47CTAB	-417475.47	-91801.32	-1076786.95	-377728.82
9SDS-1CTAB	-490772.30	-178997.90	-1148876.01	-450144.72
22SDS-2CTAB	-486293.52	-174174.76	-1144418.24	-445658.56
47SDS-5CTAB	-587575.62	-164909.12	-1144418.24	-441402.52

Table 3. The mean values of L-J interaction energy (kJ/mol) of the mixed surfactant molecules with graphene for all simulated systems.

System	300 K	600 K	NaCl	Ethanol
1SDS-9CTAB	-2237.15	-1558.28	-2298.49	-1969.14
2SDS-22CTAB	-4393.12	-2637.08	-4511.35	-4217.29
5SDS-47CTAB	-5063.21	-3006.61	-5188.37	-4958.97
9SDS-1CTAB	-1923.41	-1082.91	-1948.16	-1773.82
22SDS-2CTAB	-3792.81	-2055.85	-3953.98	-3623.01
47SDS-5CTAB	-4545.16	-2506.37	-3953.98	-4341.52

Table 4. The mean values of kinetic energy (kJ/mol) for simulated systems at 300 K and 600 K.

System	300 K	600 K
1SDS-9CTAB	102238.24	204462.90
2SDS-22CTAB	104302.45	208588.92
5SDS-47CTAB	110344.24	220679.93
9SDS-1CTAB	101601.13	203105.41
22SDS-2CTAB	102749.74	205522.23
47SDS-5CTAB	106436.81	212835.32

The altitude of this peak suggested the higher likelihood of finding the surfactant molecules at this distance than at other distances. The lower-altitude peaks suggested the lower probability of finding the molecules at the relevant distance. The negligible probability of finding surfactant molecules at very long distances is shows by g(r) approaching 0 (except systems with a temperature of 600 K).

The effect of electrolyte

The effect of electrolyte was assessed using 4M NaCl for each system. Fig. 6 shows the simulation snapshots of the mixed surfactants adsorbed onto single-layer graphene sheets in the presence of electrolyte. Comparing these snapshots with those in the absence of electrolyte showed that the surfactant molecules were positioned in parallel and formed a single-layer structure on graphene at a low and medium surface coverage. At a high surface coverage, the volume of the hemi-spherical micelles formed on graphene slightly increased in the presence of the electrolyte. By adding the electrolyte to the SDS/CTAB aqueous solution, the electrolyte ions have a screening effect on the electrostatic repulsion between the charged head groups of surfactants, such that the head groups approach each other and are drawn into the aqueous phase. This behavior of surfactants has led to volumetric expansion in the structure of hemi-spherical micelles. This observation is consistent with the observations of *Duque et al.*, who found that the electrolyte has a screening effect on the electrostatic repulsion between SDS head groups, which increases SDS adsorption on SWNTs, leading to volumetric expansion of SDS/SWNT composite structure [33].

Table 2 presents the total energy of the systems simulated in the presence and absence of electrolyte. As Table 2 shows, the total energy values for the systems in the presence of 4M NaCl electrolyte are less than the total energy values for the electrolyte-free systems, indicating better adsorption and better interactions between the particles in the electrolyte-containing systems. Table 3 presents the energy levels of L-J interactions in the mixed surfactant molecules on the graphene surface with and without the 4M NaCl solution, suggesting lower energy levels in the presence of the electrolyte, which is consistent with the simulation snapshots that showed the greater tendency of the surfactants to adsorb onto graphene in the presence of the electrolyte. Wu and Yang also showed that the addition of $CaCL_2$ electrolyte to aqueous SDS/graphene

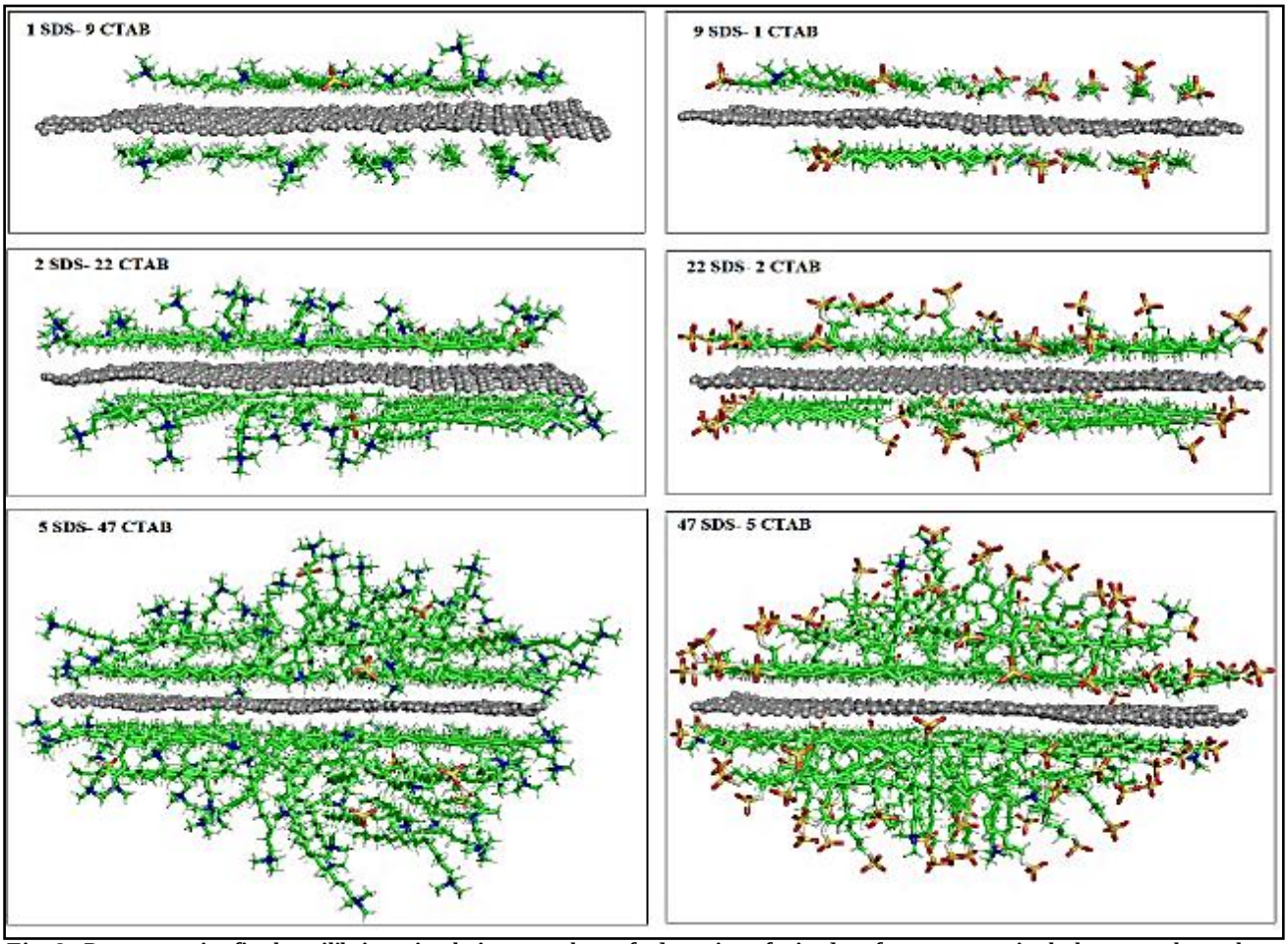

Fig. 6: Representative final equilibrium simulation snapshots of adsorption of mixed surfactants onto single-layer graphene sheets in presence of NaCl electrolyte. Water molecules and NaCl are not shown for clarity. The color code is the same as in Fig. 2.

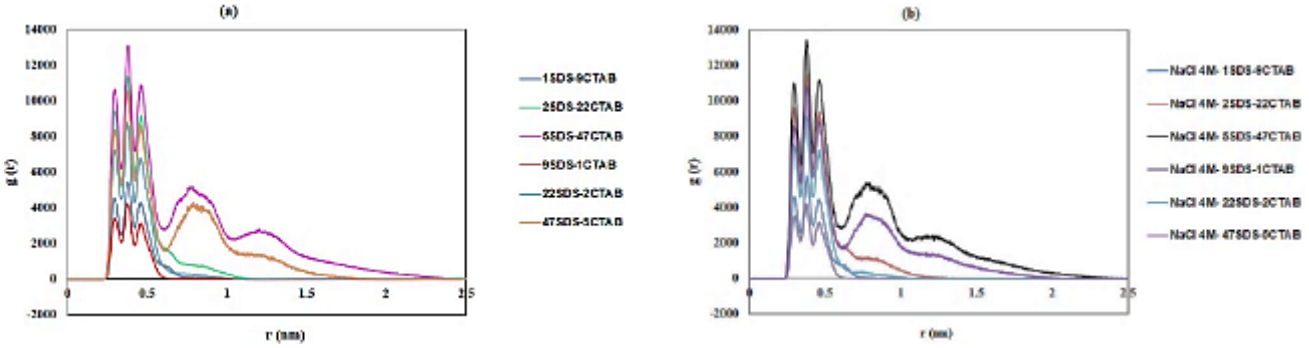

Fig. 7: Simulated radial distribution functions (RDFs) of surfactants as a function of the distance from the z-axis of the graphene in both with and without 4M NaCl.

solution strengthens the repulsive barrier of the potential mean force, which prevents the re-aggregation of graphene sheets together [63]. Table 3 shows the lower energy of interactions between the surfactant molecules and graphene at low coverage levels, which can be explained by the low concentration of the surfactant.

Fig. 7 shows the RDF of the surfactants with respect to the graphene axis with and without the electrolyte, which shows similarity between Fig. 7a with 7b. The strongest peak observed at around 0.4 nm in Fig. 7a and 7b showed the higher probability of finding the surfactant molecules at this distance compare to other distances. The subsequent

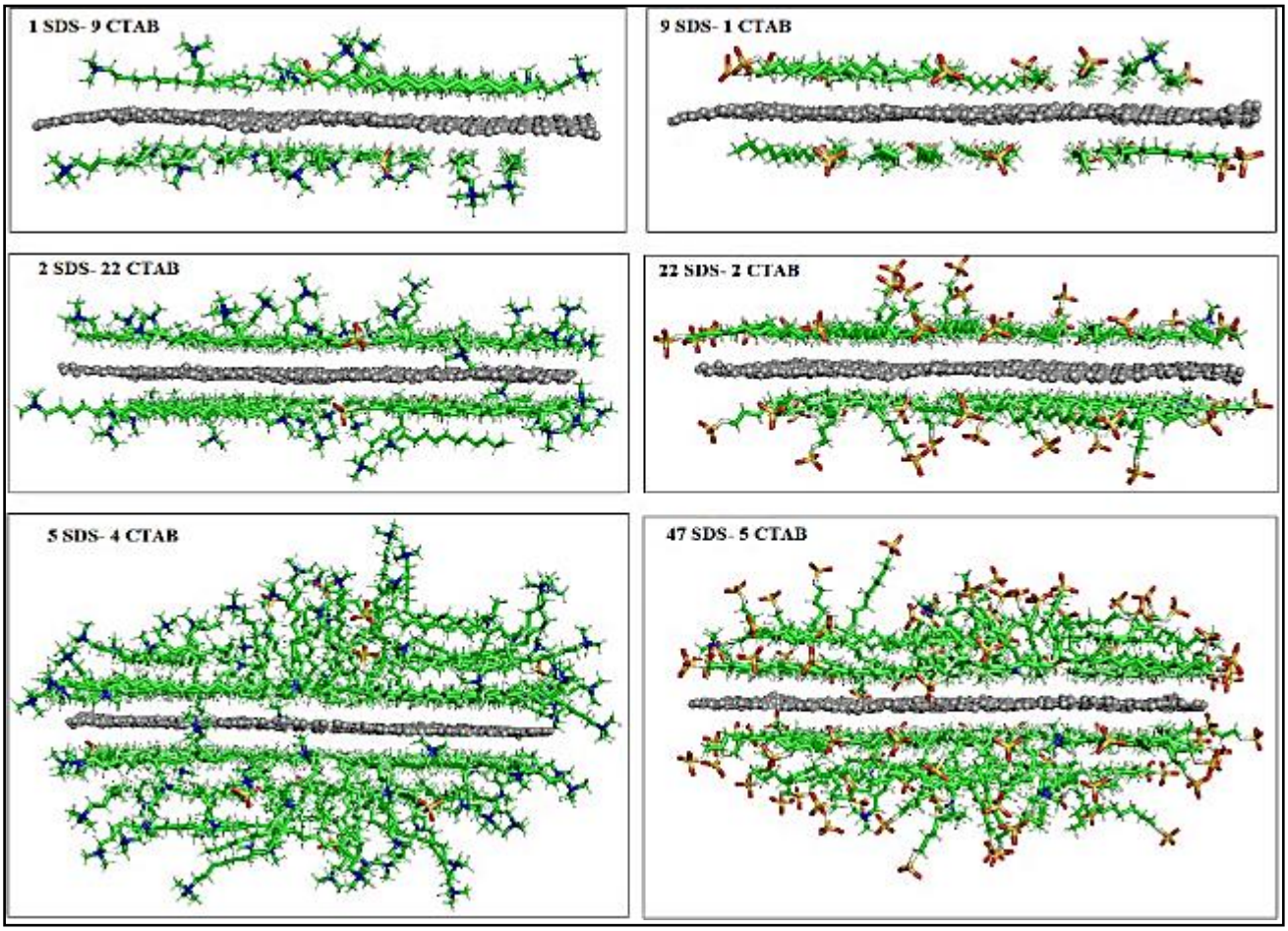

Fig. 8: Representative final equilibrium simulation snapshots of adsorption of mixed surfactants onto single-layer graphene sheets in presence of ethanol. Water molecules and ethanol are not shown for clarity. The color code is the same as in Fig. 2.

peaks at lower altitudes suggested the lower probability of being found at the relevant distances. Comparing Fig. 7a with 7b showed the higher peak altitude in the presence of 4M NaCl electrolyte, which demonstrated the higher adsorption rate in the presence of the electrolyte. The subsequent peaks at lower altitudes showed the lower probability of the molecules begin found at these distances. The negligible probability of finding surfactant molecules at very long distances is shows by g(r) approaching 0.

The effect of alcohol

Ethanol was used in the simulated systems to investigate the effect of alcohol on the adsorption of the mixed surfactants onto graphene. Fig. 8 shows the simulation snapshots of the adsorption of the mixed surfactants on single-layer graphene sheets in the aqueous solution containing ethanol and the surfactant. According to the simulation snapshots, at low and medium surface coverage levels, the surfactant molecules were positioned in parallel and formed a single-layer structure on graphene and hemi-spherical micelles formed on graphene at high coverage levels.

Table 2 presents the total energy of the simulated systems with and without ethanol, suggesting the lower energy of the majority of the simulated systems and higher stability of the systems without ethanol. In the presence of ethanol, the lower total energy of the anionic-rich systems than that of the cationic-rich systems can be explained by structural differences between CTAB and SDS molecules. Trimethylammonium in the head group of CTAB molecules applies repulsive force with ethanol molecules. Similarly, sulfate in the head group of SDS molecules develops hydrogen bonding with ethanol molecules. Similarly, the formation of hydrogen bonds between ethanol functional groups and MWCNTs functional groups causes dispersion of CNTs and stabilization of dispersed CNTs [35].

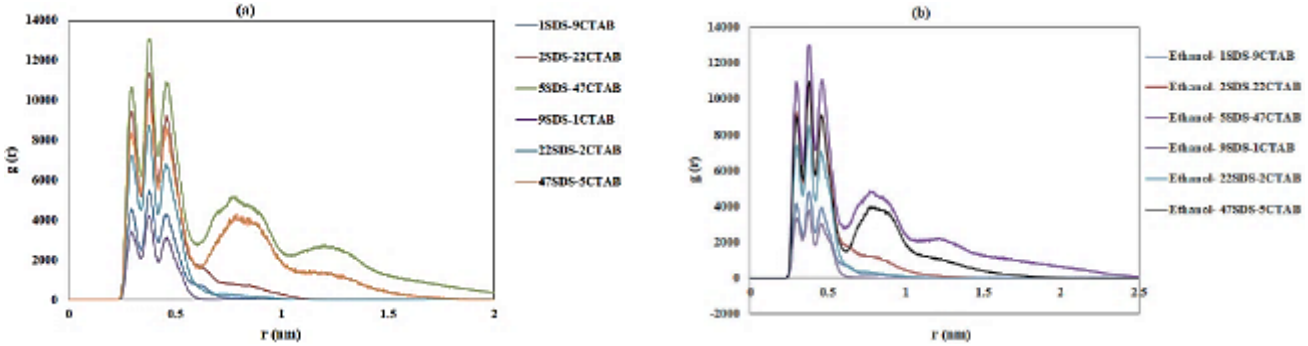

Fig. 9: Simulated radial distribution functions (RDFs) of surfactants as a function of the distance from the z-axis of the graphene (a) with ethanol and (b) without ethanol.

Furthermore, four extra methylene groups in the hydrocarbon tails of CTAB compared to SDS cause greater repulsion between CTAB and ethanol molecules. The anionic-rich systems containing ethanol were thus more stable than the cationic-rich systems. Table 3 presents the energy levels of L-J interactions between the mixed surfactant molecules on the graphene surface with and without ethanol, suggesting the lower energy and more interactions between the surfactants and graphene without ethanol. The higher energy of interactions between the mixed surfactant molecules on graphene at high coverage levels can be explained by the high concentration of the surfactants.

Fig. 9 shows the RDF of the surfactants in relation to the graphene axis with and without ethanol. Striking similarities were observed between Fig. 9a and 9b. The strongest peak with the same altitude observed at about 0.4 nm in both figures suggested the higher probability of finding the surfactant molecules at this distance than at other distances. The subsequent peaks with smaller altitudes showed the lower probability of finding the molecules at the relevant distances. The negligible probability of finding surfactant molecules at very long distances is shows by g(r) approaching 0.

CONCLUSIONS

The adsorption of mixed catationic surfactants on graphene nano-sheets was investigated using MD simulations under different solution conditions (temperature, alcohol and electrolyte). Moreover, interactions between the surfactants and graphene and morphology of the assemblies formed on graphene were also investigated. The total energy and L-J energy of the simulated systems and RDF around the graphene axis were calculated. The simulation results showed that surfactant is better adsorbed on graphene and the systems are more stable at lower temperatures. It has been observed that anionic-rich systems containing ethanol are more stable than cationic-rich systems, possibly due to the formation of a hydrogen bond between ethanol and SDS molecules. According to the RDF and calculation results of the total energy and L-J energy, adding the electrolyte to the aqueous solution of the surfactants improved their adsorption onto graphene. By adding the electrolyte to the mixed surfactants aqueous solution, the electrolyte ions have a screening effect on the electrostatic repulsion between the charged head groups of surfactants, such that the head groups approach each other and are drawn into the aqueous phase. This behavior of surfactants has led to volumetric expansion in the structure of hemi-spherical micelles.

Received: Nov. 11, 2021 ; Accepted: Apr. 4, 2022

References

[1] Novoselov K.S., Geim A.K., Morozov S.V, Jiang D., Zhang Y., Dubonos S.V, Grigorieva I.V, Firsov A.A., Electric Field Effect in Atomically Thin Carbon Films, *Science*, **306:** 666–669 (2004).

[2] Geim A.K., Novoselov K.S., The Rise of Graphene, *Nat. Mater.*, **6:** 183–191 (2007).

[3] Dasari Shareena T.P., McShan D., Dasmahapatra A.K., Tchounwou P.B., A Review on Graphene-Based Nanomaterials in Biomedical Applications and Risks in Environment and Health, *Nano-Micro Lett.*, **10:** 1-34 (2018).

[4] Reina G., González-Domínguez J.M., Criado A., Vázquez E., Bianco A., Prato M., Promises, Facts and Challenges for Graphene in Biomedical Applications, *Chem. Soc. Rev.*, **46:** 4400–4416 (2017).

[5] Narayan Banerjee A., Graphene and its Derivatives as Biomedical Materials: Future Prospects and Challenges, *Interface Focus*, **8:** 20170056 (2018).

[6] Shadjou N., Hasanzadeh M., Graphene and Its Nanostructure Derivatives for use in Bone Tissue Engineering: Recent Advances, *J. Biomed. Mater. Res. - Part A.*, **104:** 1250–1275 (2016).

[7] Basar C.A., A Mathematical Model for Adsorption of Surfactant onto Powdered Activated Carbon, *Iran. J. Chem. Chem. Eng.(IJCCE)*, **37:** 125–131 (2018).

[8] Shih C.J., Lin S., Strano M.S., Blankschtein D., Understanding the Stabilization of Liquid Phase-Exfoliated Graphene in Polar Solvents: Molecular Dynamics Simulations and Kinetic Theory of Colloid Aggregation, *J. Am. Chem. Soc.*, **132:** 14638–14648 (2010).

[9] Behabtu N., Lomeda J.R., Green M.J., Higginbotham A.L., Sinitskii A., Kosynkin D.V., Tsentalovich D., Parra-Vasquez A.N.G., Schmidt J., Kesselman E., Cohen Y., Talmon Y., Tour J.M., Pasquali M., Spontaneous High-Concentration Dispersions and Liquid Crystals of Graphene., *Nat. Nanotechnol*., **5:** 406–411 (2010).

[10] Hernandez Y., Nicolosi V., Lotya M., Blighe F.M., Sun Z., De S., McGovern I.T., Holland B., Byrne M., Gun'Ko Y.K., Boland J.J., Niraj P., Duesberg G., Krishnamurthy S., Goodhue R., Hutchison J., Scardaci V., Ferrari A.C., Coleman J.N., High-Yield Production of Graphene by Liquid-Phase Exfoliation of Graphite, *Nat. Nanotechnol*., **3:** 563–568 (2008).

[11] Ciesielski A., Samorì P., Graphene via Sonication Assisted Liquid-Phase Exfoliation, *Chem. Soc. Rev*., **43:** 381–98 (2014).

[12] Lotya M., Hernandez Y., King P.J., Smith R.J., Nicolosi V., Karlsson L.S., Blighe F.M., De S., Zhiming W., McGovern I.T., Duesberg G.S., Coleman J.N., Liquid Phase Production of Graphene by Exfoliation of Graphite in Surfactant/Water Solutions, *J. Am. Chem. Soc*., **131:** 3611–3620 (2009).

[13] Torrisi F., Carey T., Graphene, Related Two-Dimensional Crystals and Hybrid Systems for Printed and Wearable Electronics, *Nano Today.*, **23:** 73–96 (2018).

[14] Lin S., Shih C.J., Strano M.S., Blankschtein D., Molecular Insights into the Surface Morphology, Layering Structure, and Aggregation Kinetics of Surfactant-Stabilized Graphene Dispersions, *J. Am. Chem. Soc*., **133:** 12810–12823 (2011).

[15] Liu S., Wu D., Yang X., Coarse-Grained Molecular Simulation of Self-Assembly Nanostructures of CTAB on Nanoscale Graphene, *Mol. Simul.*, **42:** 31–38 (2016).

[16] Liu Y., Li R., Liang B., Li C., Hu J., Zeng K., Yang G., Bio-Adenine-Bridged Molecular Design Approach Toward Non-Covalent Functionalized Graphene by Liquid-Phase Exfoliation, *J. Mater. Sci*., **55:** 140–150 (2020).

[17] Arunachalam V., Vasudevan S., Probing Graphene-Surfactant Interactions in Aqueous Dispersions with Nuclear Overhauser Effect NMR Spectroscopy and Molecular Dynamics Simulations, *J. Phys. Chem. C*., **121:** 16637–43 (2017).

[18] Blanch A.J., Lenehan C.E., Quinton J.S., Optimizing Surfactant Concentrations for Dispersion of Single-Walled Carbon Nanotubes in Aqueous Solution, *J. Phys. Chem. B.*, **114:** 9805–11 (2010).

[19] Lotya M., King P.J., Khan U., De S., Coleman J.N., High-Concentration, Surfactant- Stabilized Graphene Dispersions, *ACS Nano,* **4:** 3155–62 (2010).

[20] Green A.A., Hersam M.C., Solution Phase Production of Graphene with Controlled Thickness via Density Differentiation, *Nano Lett,* **12:** 4031-4036 (2009).

[21] Zhang L., Zhang Z., He C., Dai L., Liu J., Wang L., Rationally Designed Surfactants for Few-Layered Graphene Exfoliation: Ionic Groups Attached to Electron-Deficient π-Conjugated Unit through Alkyl Spacers, *ACS Nano*, **8(7):** 6663–6670 (2014).

[22] Guardia L., Fernández-Merino M.J., Paredes J.I., Solís-Fernández P., Villar-Rodil S., Martínez-Alonso A., Tascón J.M.D., High-Throughput Production of Pristine Graphene in an Aqueous Dispersion Assisted by Non-Ionic Surfactants, *Carbon*, **49(5):** 1653–1662 (2011).

[23] Hardy A., Dix J., Williams C.D., Siperstein F.R., Carbone P., Bock H., Design Rules for Graphene and Carbon Nanotube Solvents and Dispersants, *ACS Nano.*, **12:** 1043–1049 (2018).

[24] Li J., Yan H., Dang D., Wei W., Meng L., Salt and Water Co-Assisted Exfoliation of Graphite in Organic Solvent for Efficient and Large Scale Production of High-Quality Graphene, *J. Colloid Interface Sci.*, **535:** 92–99 (2019).

[25] Poorsargol M., Sohrabi B., Dehestani M., Study of the Gemini Surfactants Self-Assembly on Graphene Nanosheets: Insights from Molecular Dynamic Simulation, *J. Phys. Chem. A*, **122:** 3873–3885 (2018).

[26] Díez-Pascual A.M., Vallés C., Mateos R., Vera-López S., Kinloch I.A., San Andrés M.P., Influence of Surfactants of Different Nature and Chain Length on the Morphology, Thermal Stability and Sheet Resistance of Graphene, *Soft Matter.*, **14:** 6013–6023 (2018).

[27] Vera-López S., Martínez P., San Andrés M.P., Díez-Pascual A.M., Valiente M., Study of Graphene Dispersions in Sodium Dodecylsulfate by Steady-State Fluorescence of Pyrene, *J. Colloid Interface Sci.*, **514:** 415–424 (2018).

[28] Yeon C., Lee K., Lim J.W., High-yield Graphene Exfoliation using Sodium Dodecyl Sulfate Accompanied by Alcohols as Surface-Tension-Reducing Agents in Aqueous Solution, *Carbon*, **83:** 136–143 (2014).

[29] Dubey N., Studies of Mixing Behavior of Cationic Surfactants, *Fluid Phase Equilibria.*, **368:** 51–57 (2014).

[30] Taghinezhad E., Rasooli Sharabiani V., Kaveh M., Modeling and Optimization of Hybrid HIR Drying Variables for Processing of Parboiled Paddy using Response Surface Methodology, *Iran. J. Chem. Chem. Eng.(IJCCE)*, **38:** 251–260 (2019).

[31] Poorsargol M., Alimohammadian M., Sohrabi B., Dehestani M., Dispersion of Graphene using Surfactant Mixtures: Experimental and Molecular Dynamics Simulation Studies, *Appl. Surf. Sci.*, **464:** 440–50 (2019).

[32] Stiernstedt, J., Fröberg, J.C., Tiberg, F., Rutland, M.W., Forces Between Silica Surfaces with Adsorbed Cationic Surfactants: Influence of Salt and Added Nonionic Surfactants, *Langmuir*, **21:** 1875–1883 (2005).

[33] Duque J.G., Densmore, C.G., Doorn, S.K., Saturation of Surfactant Structure at the Single-Walled Carbon Nanotube Surface, *J. Am. Chem. Soc.*, **132:** 16165–16175 (2010).

[34] Silvera-Batista, C.A., Scott, D.C., McLeod, S.M., Ziegler, K.J., A Mechanistic Study of the Selective Retention of SDS-Suspended Single-Wall Carbon Nanotubes on Agarose Gels, *J. Phys. Chem. C*, **115(19):** 9361–9369 (2011).

[35] Bricha M., Mabrouk K.E., Effect of Surfactants on the Degree of Dispersion of MWNTs in Ethanol Solvent, Colloids Surfaces, *A Physicochem. Eng. Asp.*, **561:** 57–69 (2019).

[36] Lund S., Kauppila J., Sirkiä S., Palosaari J., Eklund O., Latonen R.M., Smått J.H., Peltonen J., Lindfors T., Fast High-Shear Exfoliation of Natural Flake Graphite with Temperature Control and High Yield, *Carbon*, **174:** 123-131 (2021).

[37] Javadian S., Khosravian M., Revealing Factors Governing Self-Assembly Morphology of Fatty Acid on Graphene Synthesized by Surfactant-Assisted LPE: A Joint MD, SAPT(DFT), and Experimental Study, *J. Phys. Chem. C*, **122:** 37 (2018).

[38] Shahraki S., Samareh Delarami H., Poorsargol M., Sori Nezami Z., Structural and Functional Changes of Catalase through Interaction with Erlotinib Hydrochloride. Use of Chou's 5-Steps Rule to Study Mechanisms, *Spectrochimica Acta Part A: Molecular and Biomolecular Spectroscopy*, **260:** 119940 (2021).

[39] Vessally E., Farajzadeh P., Najafi E., Possible Sensing Ability of Boron Nitride Nanosheet and its Al– and Si–Doped Derivatives for Methimazole Drug by Computational Study, *Iran. J. Chem. Chem. Eng. (IJCCE)*, **40:** 1001-1011 (2021).

[40] Noorpoor A., Avishan M., Nazari Kudahi S., Experimental and Theoretical Investigation of CO_2 Adsorption on Amine-Modified Pumice as an Affordable Adsorbent, *Iran. J. Chem. Chem. Eng. (IJCCE)*, **40:** 1148-1161 (2021).

[41] Al-Moameri H., Zhao Y., Ghoreishi R., Suppes G., Simulation Silicon Surfactant Rule on Polyurethane Foaming Reactions, *Iran. J. Chem. Chem. Eng. (IJCCE)*, **40:** 1256-1268 (2021).

[42] Mohammad Alipour F., Babazadeh M., Vessally E., Hosseinian A., A Computational Study on the Some Small Graphene-Like Nanostructures as the Anodes in Na–Ion Batteries, *Iran. J. Chem. Chem. Eng. (IJCCE)*, **40:** 691-703 (2021).

[43] Singh S., Agnihotri N., Rathi P., Agnihotri R., Kumar V., Molecular Dynamics, Biological Study and Extractive Spectrophotometric Determination of Vanadium (V) - 2-methyl-8-quinolinol Complex, *Iran. J. Chem. Chem. Eng. (IJCCE)*, **40:** 207-214 (2021).

[44] Munir S., Khan B., Abdullah A., Khan S., Naz S., Wali Q., Tabbasam N., Computational Investigations of a Novel Charge Transfer Complex for Potential Application in Dye-Sensitized Solar Cells, *Iran. J. Chem. Chem. Eng. (IJCCE)*, **39:** 19-27 (2020).

[45] Rezazadeh Mofradnia S., Ashouri R., Abtahi N., Yazdian F., Rashedi H., Sheikhpour M., Ashrafi F., Production and Solubility of Ectoine: Biochemical and Molecular Dynamics Simulation Studies, *Iran. J. Chem. Chem. Eng. (IJCCE)*, **39:** 259-269 (2020).

[46] Ghaemi A., Vahidi O., Salehi M., Hydrogenation of 2-Ethyl-3-Propylacrolein (EPA) in a Catalytic Reactor: Experimental, Modeling and Simulation, *Iran. J. Chem. Chem. Eng. (IJCCE)*, **39:** 59-69 (2020).

[47] Abdulfatai U., Uzairu A., Uba S., Shallangwa G.A., Quantitative Structure-Properties Relationship of Lubricating Oil Additives and Molecular Dynamic Simulations Studies of Diamond-Like-Carbon (DLC), *Iran. J. Chem. Chem. Eng. (IJCCE)*, **39:** 281-295 (2020).

[48] Zhang H., Tang S., Yue H., Wu K., Zhu Y., Liu C., Liang B., Li C., Comparison of Computational Fluid Dynamic Simulation of a Stirred Tank with Polyhedral and Tetrahedral Meshes, *Iran. J. Chem. Chem. Eng. (IJCCE)*, **39:** 311-319 (2020).

[49] Kazmi S., Awan Z., Hashmi S., Simulation Study of Ionic Liquid Utilization for Desulfurization of Model Gasoline, *Iran. J. Chem. Chem. Eng. (IJCCE)*, **38**: 209-221 (2020).

[50] Yang J., Yang X., Molecular Simulation Perspective of Liquid-Phase Exfoliation, Dispersion, and Stabilization for Graphene, *Current Opinion in Colloid & Interface Science*, **20:** 339-345 (2015).

[51] Yang P., Liu F., Understanding Graphene Production by Ionic Surfactant Exfoliation: A Molecular Dynamics Simulation Study, *J. Appl. Phys.*, **116:** 014304 (2014).

[52] Hess B., Kutzner C., Van Der Spoel D., Lindahl E., GROMACS 4: Algorithms for Highly Efficient, Load-Balanced, and Scalable Molecular Simulation, *J. Chem. Theory Comput.*, **4:** 435–447 (2008).

[53] Jorgensen W.L., Maxwell D.S., Tirado-Rives J., Development and Testing of the OPLS All-Atom Force Field on Conformational Energetics and Properties of Organic Liquids, *J. Am. Chem. Soc.*, **118:** 11225–11236 (1996).

[54] Berendsen H.J.C., Grigera J.R., Straatsma T.P., The Missing Term in Effective Pair Potentials, *J. Phys. Chem.*, **91:** 6269–6271 (1987).

[55] Darden T., York D., Pedersen L., Particle mesh Ewald: An N·log(N) method for Ewald sums in large systems, *J. Chem. Phys.*, **98:** 10089 (1993).

[56] Nosé S., A Molecular Dynamics Method for Simulations in the Canonical Ensemble, *Mol. Phys.*, **52:** 255–268 (1984).

[57] Verlet L., Computer "Experiments" on Classical Fluids. I. Thermodynamical Properties of Lennard, -Jones Molecules, *Phys. Rev.*, **159:** 98 (1967).

[58] Parrinello M., Rahman A., Polymorphic Transitions In Single Crystals: A New Molecular Dynamics Method, *J. Appl. Phys.*, **52:** 7182–7190 (1981).

[59] Martínez L., Andrade R., Birgin E.G., Martínez J.M., PACKMOL: a Package for Building Initial Configurations for Molecular Dynamics Simulations, *J. Comput. Chem.*, **30:** 2157–2164 (2009).

[60] Xu Z., Yang X., Yang Z., A Molecular Simulation Probing of Structure and Interaction for Supramolecular Sodium Dodecyl Sulfate/Single-Wall Carbon Nanotube Assemblies, *Nano Lett.*, **10:** 985–991 (2010).

[61] Tummala N.R., Striolo A., Role of Counterion Condensation in the Self-Assembly of SDS Surfactants at the Water-Graphite Interface, *J. Phys. Chem. B.*, **112:** 1987–2000 (2008).

[62] Humphrey W., Dalke A., Schulten K., VMD: Visual Molecular Dynamics, *J. Mol. Graph.*, **14:** 33–38 (1996).

[63] Wu B., Yang X., Molecular Simulation of Electrolyte-Induced Interfacial Interaction between Sds/Graphene Assemblies, *J. Phys. Chem. C.*, **117:** 23216–23223 (2013).

[64] Haile J.M., "Molecular Dynamics Simulation: Elementary Methods" John Wiley and Sons (1992).

[65] Atkins P., and de Paula J., "Physical Chemistry for the Life Sciences" New York, N.Y. W. H. Freeman Company, 469-472 (2006).